

Title	Stable elasticity of epitaxial Cu thin films on Si
Author(s)	Nakamura, N.; Ogi, H.; Hirao, M.
Citation	Physical Review B - Condensed Matter and Materials Physics. 2008, 77(24), p. 245416-1-245416-6
Version Type	VoR
URL	https://hdl.handle.net/11094/84178
rights	Copyright 2008 by the American Physical Society
Note	

Osaka University Knowledge Archive : OUKA

<https://ir.library.osaka-u.ac.jp/>

Osaka University

Stable elasticity of epitaxial Cu thin films on Si

N. Nakamura,* H. Ogi, and M. Hirao

Graduate School of Engineering Science, Osaka University, Machikaneyama 1-3, Toyonaka, Osaka 560-8531, Japan

(Received 18 December 2007; revised manuscript received 14 May 2008; published 11 June 2008)

In epitaxial films, large elastic strain originating from the lattice misfit with the substrate remains, and it could affect the elastic stiffness. However, we found that epitaxially grown Cu thin films on (001) Si show exceptionally stable stiffness: the average out-of-plane elastic constant throughout the film thickness was independent of the film thickness and of the annealing procedure up to 150 °C. We calculated the strain dependence of the elastic constants using the higher-order elastic constants and confirmed that the misfit strain with the substrate hardly affects the stiffness in the particular case of Cu(001) thin films.

DOI: [10.1103/PhysRevB.77.245416](https://doi.org/10.1103/PhysRevB.77.245416)

PACS number(s): 62.25.-g, 43.58.+z

I. INTRODUCTION

Physical properties of thin films attract many researchers because they are often different from those of bulk materials, and anomalous properties often allow development of high-performance devices. Elastic stiffness is one of the fundamental physical properties, and the thin-film elastic stiffness has been considered to be different from that of bulk material. In polycrystalline films, defects such as nanocracks, point defects, dislocations, and incohesive-bonding regions at the grain boundaries make the elastic stiffness smaller than the defect-free bulk material's stiffness.¹⁻⁵ On the other hand, some studies reported enhanced elastic stiffness in superlattice thin films, which was attributed to a large strain originating from the lattice misfit at interfaces between the elements.^{6,7} Recently, complicated thickness behavior of the stiffness was observed in metallic films,⁸⁻¹⁰ where the stiffness significantly depended on the film thickness. Thus, thin-film stiffness varies depending on the thickness, substrate, deposition condition, annealing condition, and so on, and it has been recognized to be unstable.

However, in this study, we confirmed stable elastic modulus of epitaxial (001) Cu films deposited on monocrystal (001) Si substrates by laser acoustic-phonon-resonance spectroscopy. The laser acoustic-phonon resonance spectroscopy determines the average out-of-plane modulus throughout the thickness of thin films. The stiffness of the epitaxial Cu film is independent of its thickness in the range of 16–90 nm, showing approximately the same value as that of the bulk Cu. Furthermore, it is not affected by the post-annealing procedure at up to 150 °C. Considering that epitaxially grown thin films show fine crystallinity and include few defects, this stable elasticity is an expected result. However, we have to note that such a heterogeneous epitaxial film possesses large *elastic* strain originating from the lattice misfit with the substrate; the strain reaches of the order of 10^{-2} at the interface, which will not occur in the bulk material because of dislocation movements. It is expected that a large elastic strain changes the elastic stiffness according to anharmonic interatomic potential.^{11,12} However, our observation contradicts this prediction.

Cu is a familiar material, and Cu thin film is extensively used as a metallization material in many devices, owing to its favorable electric conductivity and high tolerance to elec-

tromigration. However, its elastic property has not been reported in detail because of the difficulty of measuring the thin-film elastic stiffness. In previous studies, the stiffness of thin films was measured by gripping the specimens to stretch or bend them.^{1,3} The gripping condition seriously affected the resultant stiffness, and quantitative evaluation has been difficult. Alternatively, the Brillouin scattering method contactlessly estimated the frequency of acoustic phonons in thin films, and standing waves in the thickness direction was observed,¹³⁻¹⁵ which enables to determine the out-of-plane elastic constants, as well as the laser acoustic-phonon resonance spectroscopy. Brillouin scattering is applicable for transparent or translucent materials, whereas the acoustic-phonon resonance spectroscopy is for opaque materials. Therefore, when metallic thin films are studied, the latter is efficient.

II. LASER ACOUSTIC-PHONON RESONANCE SPECTROSCOPY

For determining the reliable elastic stiffness of ultrathin films, we have developed the laser acoustic-phonon resonance spectroscopy.⁸ When an ultrashort light pulse (~ 100 fs) irradiates the film surface, acoustic phonons are excited, and nonpropagated modes remain to develop into standing waves. Their resonance frequencies f_n are determined by $f_n = n\sqrt{C/\rho}/(2d)$ when the acoustic impedance of the film is larger than that of the substrate. Here, d , ρ , n , and C are the film thickness, mass density, integer indicating the resonance mode, and the elastic stiffness associated with the longitudinal wave propagating along the film-thickness direction, respectively. The oscillations were detected by monitoring the intensity of the delayed probe beam reflected at the film surface because the reflectivity is changed by the strain at the film surface.¹⁶ Here, we have to note that the laser acoustic-phonon resonance spectroscopy determines the *average* elastic stiffness in the film-thickness direction.

Figure 1 shows the typical responses of the time-resolved reflectivity variation and the corresponding Fourier spectra. Observed signals consist of two oscillations. The low-frequency oscillation originates from the acoustic-phonon resonance within the Cu film, whose frequency changes with the film thickness. The second (high-frequency) oscillation (Brillouin oscillation) is generated by interference between

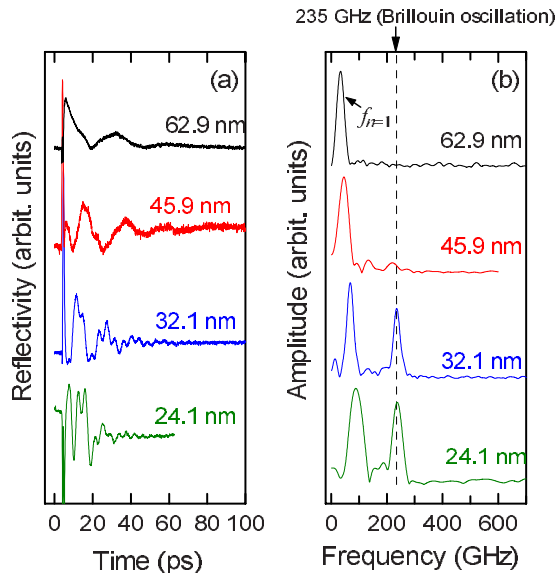


FIG. 1. (Color online) (a) Oscillations of the reflectivity from epitaxially-grown Cu thin films on Si substrates. (b) Fourier spectra of the corresponding responses.

the light reflected at the substrate surface and the light diffracted by the acoustic wave propagating in the substrate.¹⁷ This oscillation frequency is given by $2mv/\lambda$ for the normal incident light, where m , v , and λ denote the refractive index and the sound velocity in the substrate, and the wavelength of the light, respectively. By using bulk material's values for them, we predict the oscillation frequency of 235 GHz,⁹ which agrees well with the peak observed in the spectra. The signal from Brillouin oscillation becomes small as the film thickness increases because the reflectivity at the film increases with the film thickness, and the probe light cannot penetrate into the substrate. For example, in the case of epitaxial Cu films, the signal from Brillouin scattering disappeared when the film thickness was larger than 45.9 nm [Fig. 1(b)].

The other peaks thus indicate the resonance frequencies of acoustic phonons. In the laser acoustic-phonon resonance spectroscopy, acoustic phonons are simultaneously generated at the same time throughout the film-thickness direction. Among them, the fundamental standing wave ($n=1$) was preferentially detected because of high attenuation of higher-frequency modes ($n=2, 3, \dots$). We determined the elastic stiffness from the resonance frequency of the fundamental mode using the bulk mass density, and the film thickness determined by the x-ray reflectivity measurements.^{18,19} Noteworthy point of this technique is that we can contactlessly determine the elastic stiffness without ambiguous parameters; we need only the film thickness, mass density, and the resonance frequency. This feature enables accurate measurements of thin-film elastic stiffness.

III. SPECIMEN

Cu thin films were deposited on the (001) plane of monocrystal Si substrates by the RF magnetron sputtering.

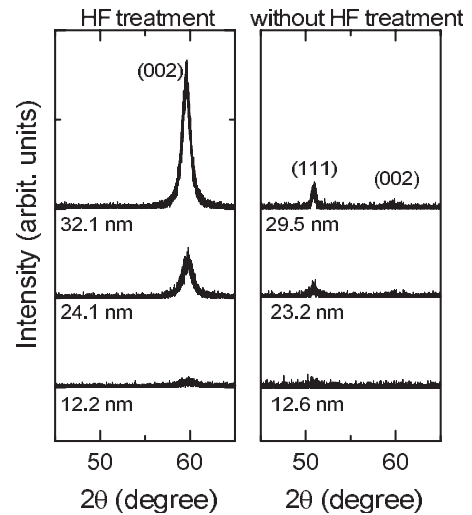


FIG. 2. X-ray diffraction spectra in high-angle regions of Cu thin films deposited on Si(001) with or without HF treatment (Co $K\alpha$).

Two kinds of substrates were prepared: (i) (001)Si covered with the natural oxide and (ii) (001)Si etched by hydrofluoric acid (10% HF) for 60 s at room temperature to remove the natural oxide. By removing the oxide, the predominant crystallographic orientation of the deposited Cu films in the film thickness direction changed from $\langle 111 \rangle$ to $\langle 001 \rangle$ (Fig. 2). Here, we express them as Cu(111)/Si and Cu(001)/Si specimens, respectively. For Cu(001)/Si specimens, the diffraction peak from Cu(002) plane was observed even if the film was thinner than 12 nm. However, for Cu(111)/Si specimens thinner than 20 nm, we did not observe any diffraction peaks. This result indicates well-developed crystallinity of Cu(001)/Si specimens comparing to the Cu(111)/Si specimens. When the film thickness of Cu(111)/Si specimens was larger than 60 nm, we observed diffraction peaks from (111) and (002) planes, which indicates that Cu(111)/Si specimens are polycrystalline.

We confirmed the epitaxial growth of Cu(001)/Si by the in-plane x-ray diffraction measurement. We set the detector to detect the diffracted beam from Cu(200) planes, and the specimen was rotated around the film-thickness direction. Then, the same measurement was made for the Si(400) planes by changing the detector's position. During one revolution of the specimen, four diffraction peaks were observed for Cu(200) and Si(400) (Fig. 3). This result indicates that the Cu(001)/Si shows fourth-order rotational symmetry about the thickness direction, and epitaxial growth of Cu film is confirmed. Furthermore, difference of diffraction angle by 45° between Cu(200) and Si(400) indicates that Cu(001) film is grown epitaxially with a 45° in-plane rotation about the $\langle 001 \rangle$ direction of Si.

IV. RESULTS

For comparison to the measured elastic constants, we calculated the longitudinal-wave moduli along $\langle 100 \rangle$ and $\langle 111 \rangle$ directions using the elastic stiffness C_{ij} of the monocrystal

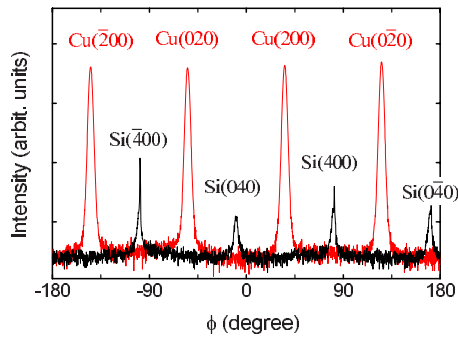


FIG. 3. (Color online) In-plane x-ray diffraction spectra from the epitaxial Cu film and Si substrate of Cu(001)/Si specimen. The film thickness is 45 nm (Co K α). Horizontal axis is the rotation angle of the specimen around the film-thickness direction.

bulk Cu, ($C_{11}=167.0$ GPa, $C_{12}=120.9$ GPa, and $C_{44}=74.64$ GPa),²⁰ and obtained $C_{\text{bulk}}^{(001)}=C_{11}=167.0$ GPa and $C_{\text{bulk}}^{(111)}=(C_{11}+2C_{12}+4C_{44})/3=235.8$ GPa, respectively. They are the possible maximum moduli without any defects, and we define them as the standard moduli for Cu(001)/Si and Cu(111)/Si, respectively.

Figure 4 shows the thickness dependence of the stiffness, normalized by the standard modulus, and that of the strain S_{\perp} in the out-of-plane direction. Before the deposition, the interatomic distance between (100) planes in a bulk Cu plate was determined by the x-ray diffraction measurement, and it was defined as the standard interatomic distance of the unstrained Cu. S_{\perp} was then determined from the standard value and out-of-plane interatomic distance of thin films. In Fig. 4, the stiffness of Cu(001)/Si is independent of the film thickness, and it is comparable with the standard modulus, while the stiffness of Cu(111)/Si is smaller than the standard modulus by 20%. Furthermore, Cu films shrink in the out-of-plane direction (elongate in the plane) for both Cu(001)/Si and Cu(111)/Si; S_{\perp} of Cu(001)/Si was negative, and its absolute value increased as the film thickness decreased, while S_{\perp} of

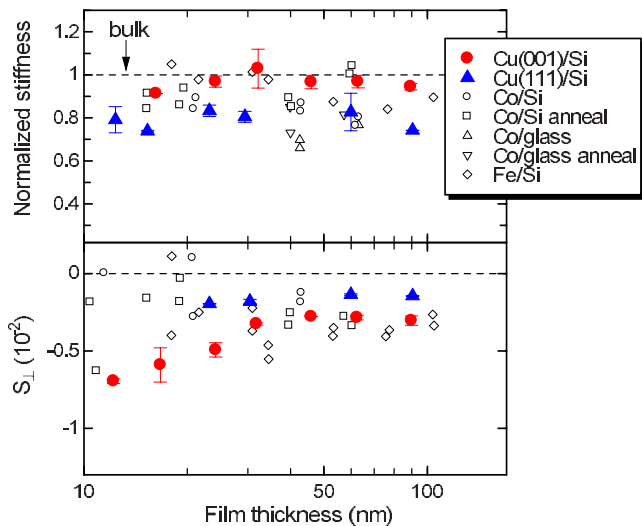


FIG. 4. (Color online) Thickness dependence of the out-of-plane modulus C and the out-of-plane strain S_{\perp} of Cu(001)/Si, Cu(111)/Si, Co/Si, Co/glass, and Fe/Si.

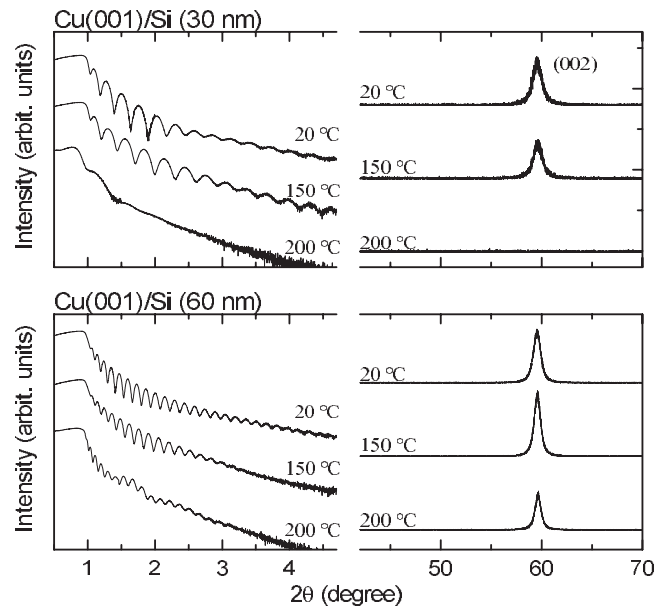


FIG. 5. X-ray reflectivity changes (left) and x-ray diffraction spectra (right) of Cu(001)/Si specimens at different annealing temperatures (Co K α).

Cu(111)/Si appears independent of the thickness.

Next, we investigated the effect of the post annealing treatment on the stiffness and internal structure. This annealing treatment was carried out just after the deposition in vacuum for 30 min. Figure 5 shows x-ray diffraction spectra of Cu(001)/Si specimens at low and high angle regions. In the low-angle region, an oscillation pattern is caused by the interference of x-rays reflected at the surface and at the interface. When the annealing temperature reaches 200 °C, the oscillation pattern diminishes, and in 30-nm thick Cu(001)/Si it becomes invisible. In high-angle regions, the diffraction peak from Cu(001) also diminishes and disappears as the annealing temperature increases. These results indicate that the post annealing treatment causes the interdiffusion to generate a second phase, making roughened interface. However, when the annealing temperature is below 150 °C, the oscillation pattern and the diffraction peak are clearly observed. Therefore, the interdiffusion barely occurs by the post-annealing below 150 °C, and its effect on the elastic constants is negligibly small compared with the measurement errors in the film thickness. On the other hand, significant temperature dependence of the x-ray diffraction spectrum was not observed for Cu(111)/Si.

Figure 6 shows the annealing-temperature dependences of the elastic stiffness and S_{\perp} . Although the stiffness of Cu(111)/Si specimens increases as the annealing temperature increases, that of Cu(001)/Si remains unchanged. The post annealing treatment increased the magnitude of S_{\perp} in Cu(001)/Si, and the stiffness was expected to be changed. However, the stiffness of Cu(001)/Si was not affected by the annealing procedure.

V. DISCUSSION

We observed that Cu(001) films grow epitaxially on Si substrate by the x-ray diffraction measurements, and they

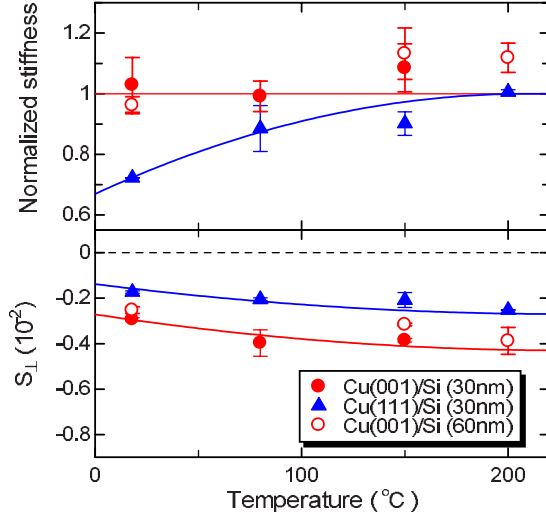


FIG. 6. (Color online) Changes in the out-of-plane modulus C (upper) and S_{\perp} (bottom) at different annealing temperatures. Film thickness is near 30 nm and 60 nm.

shrink in the thickness direction. Because the in-plane interatomic distance of Si is larger than that of Cu by 6.2%, Cu is extended biaxially in the in-plane direction, which decreases the interatomic distance normal to the film surface because of Poisson's effect. Considering that x-ray diffraction measurements determine the average strain in the film, the magnitude of the measured S_{\perp} should decrease as the film thickness increases because the in-plane strain in Cu (001) becomes maximum at the interface with the substrate, and it decreases as the distance from the interface increases. Observed film-thickness dependence of S_{\perp} shows the same trend as this prediction, and we attribute it to the distribution of strain along the thickness direction. For polycrystalline thin films, residual stress originates from several factors such as the mismatch in the thermal expansion coefficient between the film and substrate, coalescence of grains, and diffusion of sputtered atoms into the grain boundaries,^{21,22} and it has been reported that the in-plane residual stress easily changes depending on the film thickness. However, S_{\perp} of the Cu film was independent of the film thickness.

Magnitude of observed S_{\perp} of Cu(001)/Si specimen is significantly larger than that of Cu(111)/Si, which makes one expect the significant change in the stiffness because of anharmonic interatomic potential. However, the elastic stiffness of Cu(001)/Si is comparable to the stiffness of the bulk Cu, being independent of the strain. This is an interesting result. On the other hand, the elastic stiffness of the as-deposited Cu(111)/Si is significantly smaller than the predicted value. This is the general elastic behavior of the thin films, and it is often attributed to the micro- or nanodefects, and amorphous phases at grain boundaries, because the macroscopic elastic stiffness of polycrystalline thin films are sensitive to the bonding condition at the grain boundaries,²³ where the amorphous phases and incohesive bonds appear. For comparison, the elastic stiffness and S_{\perp} of Co and Fe thin films measured by the same method were shown in Fig. 4. Their elastic moduli are different from the bulk values, and compared to them, the stability of the stiffness of Cu(001)/Si is remarkable.

For understanding the unchanged elastic stiffness of the epitaxial Cu films, we discuss the strain dependence of elastic stiffness using the third-order elastic constants. In this calculation, we assume that the thin films are extended biaxially along the in-plane directions, and they shrink in the film-thickness direction because of Poisson's effect.

Thurston and Brugger¹² formulated the equation for propagation velocities of small-amplitude waves in a homogeneously deformed solid as

$$\rho_0 W^2 U_i = w_{ij} U_j. \quad (1)$$

Solving this equation, we can calculate the strain dependence of the elastic constant. Here, ρ_0 , W , and U_i denote the mass density at the unstrained state, the natural sound velocity, and the natural displacements, respectively. Then, $\rho_0 W^2$ corresponds to the governing elastic constant, and they are eigenvalues of the second-rank tensor w_{ij} given by

$$w_{ij} = N_k N_l [\delta_{ij} \tilde{t}_{kl} + (\delta_{mj} + 2\eta_{mj}) \tilde{c}_{ikml}]. \quad (2)$$

Here, $\tilde{t}_{ij} = c_{ijkl}^0 \eta_{kl} + C_{ijklmn} \eta_{kl} \eta_{mn} / 2$ and $\tilde{c}_{ijkl} = c_{ijkl}^0 + C_{ijklmn} \eta_{mn}$; c_{ijkl}^0 and C_{ijklmn} are the second-order elastic constants at unstrained state and the third-order elastic constants, respectively. N_i is the unit vector along the propagation direction. η_{ij} denotes the homogeneous Lagrangian strains. Thus, using reported values of c_{ijkl}^0 and C_{ijklmn} ,²⁴ we calculated the changes of the elastic stiffness in the biaxial strain field.

In Cu thin films, the in-plane biaxial strain will vary along the film-thickness direction; it will decrease as the distance from the interface increases. In addition, when weak-bonding regions exist in the film, the strain distribution becomes more complicated. However, the in-plane tensile strain cannot be completely released by such inclusions, and the in-plane tensile strain remains; this view is supported by the compressive strain observed by the x-ray diffraction measurements. For these reasons, we assumed that the uniform biaxial stress is applied in the in-plane directions to simplify the analysis, and the modulus $C^{(ijk)}$, regarding to the longitudinal wave propagating in the $\langle ijk \rangle$ direction, was calculated. Considering that measured elastic constant is an average value throughout the film-thickness direction, this assumption is appropriate. When epitaxial Cu thin film is considered, the uniform biaxial stress is applied along [100] and [010] directions. When polycrystalline Cu grows on the Si substrate, grains are randomly oriented along the in-plane direction. We then calculated elastic constants in [111] direction by applying the stress in $[1\bar{1}0]$ and $[11\bar{2}]$ directions.

Figure 7 shows the relationship between the out-of-plane strain S_{\perp} and the relative change of $C^{(ijk)}$ for the common metals, and the strain dependences of the modulus of fcc metals are also compared to the lattice parameter. Interestingly, $C^{(001)}$ of Cu hardly depends on S_{\perp} , compared to the other metals; the stable elasticity appears only for the $C^{(001)}$. Furthermore, we found that the sensitivity of the longitudinal stiffness in the $\langle 001 \rangle$ direction to the strain correlates with the lattice parameter for fcc metals; as the lattice parameter becomes small, strain dependence of $C^{(001)}$ becomes remarkable. However, Cu (001) does not obey this trend. This disagreement will include important knowledge for understand-

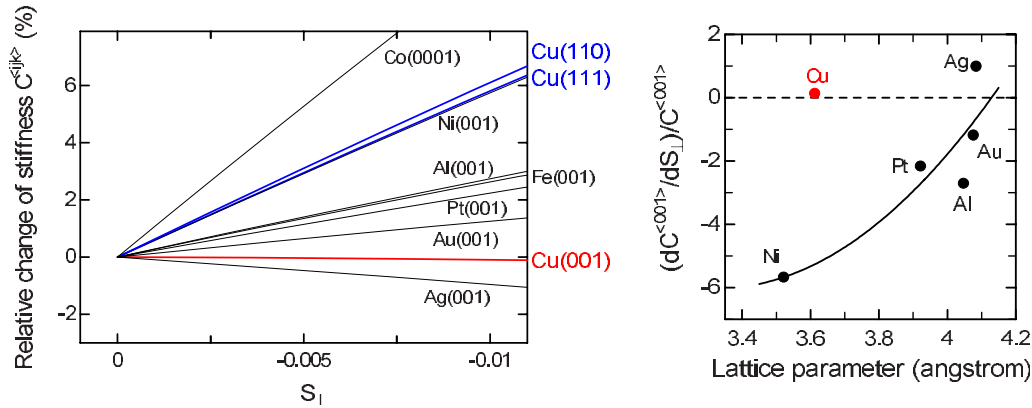


FIG. 7. (Color online) Calculated strain dependence of the longitudinal-wave modulus $C^{(ijk)}$ for various metals. (Left) Dependence of the modulus $C^{(ijk)}$ on the out-of-plane strain S_{\perp} calculated using the third-order elastic constants for the in-plane biaxial strain field. (Right) Relationship between the lattice parameter and the strain-dependence of $C^{(001)}$ of fcc metals.

ing the unexpectedly stable $C^{(001)}$ of Cu thin film, and its origin represents an important future research topic.

Considering the strain dependence of the stiffness of Cu (001) calculated in Fig. 7, Cu(111)/Si specimens would be stiffened, while the measurements showed elastic stiffness lower than the unstrained-bulk Cu. However, as mentioned above, elastic stiffness of polycrystalline thin films are sensitive to the bonding condition at the grain boundaries. Local amorphous phase and nanodefects are possible reasons for the weak bonding at the grain boundaries, and we consider that this softening effect exceeds acoustoelastic effect with the biaxial stress field.

VI. CONCLUSIONS

We conclude that stable elasticity of epitaxial Cu(001) films originates from its single crystal structure and the in-

sensitivity of Cu (001) to the biaxial deformation. This stability is important knowledge in the industrial field because the insensitive elasticity of thin films makes the design of the devices simple. Considering that the elastic properties of thin films are still uncertain and there are many combinations of film and substrate, there must be unidentified anomalies in the epitaxial thin films, and this study will lead to further investigations of the elastic constants of thin films.

ACKNOWLEDGMENTS

We are grateful to K. Tsujino and M. Matsumura, Osaka University, for the support of the hydrofluoric-acid treatments.

*nobutomo@me.es.osaka-u.ac.jp

¹D. Faurie, P.-O. Renault, E. Le Bourhis, and Ph. Goudeau, *J. Appl. Phys.* **98**, 093511 (2005).
²Z. H. Shen, P. Hess, J. P. Huang, Y. C. Lin, K. H. Chen, L. C. Chen, and S. T. Lin, *J. Appl. Phys.* **99**, 124302 (2006).
³M. C. Salvadori, I. G. Brown, A. R. Vaz, L. L. Melo, and M. Cattani, *Phys. Rev. B* **67**, 153404 (2003).
⁴N. Nakamura, H. Ogi, and M. Hirao, *Acta Mater.* **52**, 765 (2004).
⁵H. Ogi, N. Nakamura, H. Tanei, R. Ikeda, M. Hirao, and M. Takemoto, *Appl. Phys. Lett.* **86**, 231904 (2005).
⁶W. M. C. Yang, T. Tsakalakos, and J. E. Hilliard, *J. Appl. Phys.* **48**, 876 (1977).
⁷D. Baral, J. B. Ketterson, and J. E. Hilliard, *J. Appl. Phys.* **57**, 1076 (1985).
⁸H. Ogi, M. Fujii, N. Nakamura, T. Shagawa, and M. Hirao, *Appl. Phys. Lett.* **90**, 191906 (2007).
⁹H. Ogi, M. Fujii, N. Nakamura, T. Yasui, and M. Hirao, *Phys. Rev. Lett.* **98**, 195503 (2007).
¹⁰N. Nakamura, H. Ogi, T. Yasui, M. Fujii, and M. Hirao, *Phys. Rev. Lett.* **99**, 035502 (2007).

¹¹Y. H. Pao, W. Sachse, and H. Fukuoka, *Physical Acoustics* (Academic, New York, 1984), Vol. XVII.
¹²R. N. Thurston and K. Brugger, *Phys. Rev.* **133**, A1604 (1964).
¹³X. Zhang, R. Sooryakumar, A. G. Every, and M. H. Manghnani, *Phys. Rev. B* **64**, 081402(R) (2001).
¹⁴X. Zhang, R. S. Bandhu, R. Sooryakumar, and B. T. Jonker, *Phys. Rev. B* **67**, 075407 (2003).
¹⁵X. Zhang, R. Sooryakumar, and K. Bussmann, *Phys. Rev. B* **68**, 115430 (2003).
¹⁶C. Thomsen, J. Strait, Z. Vardeny, H. J. Maris, J. Tauc, and J. J. Hauser, *Phys. Rev. Lett.* **53**, 989 (1984).
¹⁷A. Devos and R. Côte, *Phys. Rev. B* **70**, 125208 (2004).
¹⁸H. Kiessig, *Ann. Phys.* **10**, 769 (1931).
¹⁹L. G. Parratt, *Phys. Rev.* **95**, 359 (1954).
²⁰H. Ogi, H. Ledbetter, S. Kim, and M. Hirao, *J. Acoust. Soc. Am.* **106**, 660 (1999).
²¹D. Winau, R. Koch, A. Führmann, and K. H. Rieder, *J. Appl. Phys.* **70**, 3081 (1991).
²²E. Chason, B. W. Sheldon, L. B. Freund, J. A. Floro, and S. J. Hearne, *Phys. Rev. Lett.* **88**, 156103 (2002).
²³H. Tanei, N. Nakamura, H. Ogi, M. Hirao, and R. Ikeda, *Phys.*

Rev. Lett. **100**, 016804 (2008).

$^{24}c_{ijkl}^0$ and C_{ijklmn} of Ag, Al, Au, Cu, and Fe are from H. Ledbetter and S. Kim, in *Handbook of Elastic Properties of Solids, Liquids, and Gases*, edited by M. Levy, H. Bass, and R. Stern

(Academic, New York, 2001), Vol. II; C_{ijklmn} of Pt and Ni are from S. Mathur and P. Gupta, *Acustica* **31**, 114 (1974); c_{ijkl}^0 and C_{ijklmn} of Co are from Y. K. Yogurtçu, G. A. Saunders, and P. C. Riedi, *Philos. Mag. A* **52**, 833 (1985).